A functional calcium-binding site in the metalloprotease domain of ADAMTS13

Michelle D. Gardner,[1] Chan K. N. K. Chion,[1] Rens de Groot,[1] Anuja Shah,[1] James T. B. Crawley,[1] and David A. Lane[1]

[1]Department of Haematology, Imperial College London, London, United Kingdom

ADAMTS13 regulates the multimeric size of von Willebrand factor (VWF). Its function is highly dependent upon Ca^{2+} ions. Using the initial rates of substrate (VWF115, VWF residues 1554-1668) proteolysis by ADAMTS13 preincubated with varying Ca^{2+} concentrations, a high-affinity functional ADAMTS13 Ca^{2+}-binding site was suggested with $K_{D(app)}$ of 80 μM (± 15 μM) corroborating a previously reported study. When Glu83 or Asp173 (residues involved in a predicted Ca^{2+}-binding site in the ADAMTS13 metalloprotease domain) were mutated to alanine, Ca^{2+} dependence of proteolysis of the substrate was unaffected. Consequently, we sought and identified a candidate Ca^{2+}-binding site in proximity to the ADAMTS13 active site, potentially comprising Glu184, Asp187, and Glu212. Mutagenesis of these residues within this site to alanine dramatically attenuated the $K_{D(app)}$ for Ca^{2+} of ADAMTS13, and for D187A and E212A also reduced the V_{max} to approximately 25% of normal. Kinetic analysis of the Asp187 mutant in the presence of excess Ca^{2+} revealed an approximately 13-fold reduction in specificity constant, k_{cat}/K_m, contributed by changes in both K_m and k_{cat}. These results were corroborated using plasma-purified VWF as a substrate. Together, our results demonstrate that a major influence of Ca^{2+} upon ADAMTS13 function is mediated through binding to a high-affinity site adjacent to its active site cleft. (Blood. 2009;113:1149-1157)

Introduction

von Willebrand factor (VWF) is a large multidomain glycoprotein that circulates in plasma as covalently associated multimers of varying size (2-40 VWF units).[1] VWF has 2 major hemostatic functions: (1) to form a bridge between the damaged vessel wall and platelets; and (2) as a carrier protein for factor VIII.[1,2] The first hemostatic event following disruption of the endothelium involves VWF binding to exposed matrix proteins. Normally, VWF circulates in plasma in a globular form. However, once bound to subendothelial collagen, the shear forces exerted by the flowing blood cause VWF to unfold and in turn adopt an elongated conformation. In this form, VWF binds to the GPIb-IX-V receptor complex on the surface of circulating platelets, resulting in their tethering and the ultimate formation of a primary platelet plug.[1,3] Large VWF multimers are more adhesive than smaller forms because they contain more platelet- and collagen-binding sites and more readily unravel in response to shear forces. VWF multimers are synthesized intracellularly in a 2-stage process—first by dimerization in the endoplasmic reticulum and then by multimerization of these dimers in the Golgi apparatus.[4] Following their secretion from endothelial cells, VWF multimers can be converted to a smaller, less adhesive form by the plasma metalloprotease, ADAMTS13.[5-10]

ADAMTS13 is expressed predominantly in the liver.[11] It has also been shown to be expressed in hepatic stellate cells,[12] in platelets,[13] by cultured endothelial cells,[14,15] and by glomerular podocytes.[16] It is secreted into the blood as an active enzyme and circulates at a plasma concentration of approximately 5 nM.[11,17,18] ADAMTS13 cleaves VWF at a single site in its A2 domain at the Tyr1605-Met1606 bond.[19-21] Physiologically, this can only occur once VWF has first been unraveled in response to rheologic shear forces. In vitro, cleavage of multimeric VWF by ADAMTS13 requires denaturants or flow/shear to enable access of the metalloprotease to the A2 domain scissile bond.[8] The lower-molecular-weight VWF multimers that arise following proteolysis exhibit reduced adhesive potential.[5] In this way, ADAMTS13 modulates VWF platelet-tethering function.

The domain structure of ADAMTS13 comprises a metalloprotease domain, disintegrin-like domain, thrombospondin type 1 repeat, cysteine-rich domain, and spacer domain, characteristic of all ADAMTS family members. Thereafter, 7 additional thrombospondin type 1 repeats occur, followed by 2 C-terminal CUB domains.[6,22] The VWF-cleaving function of ADAMTS13 is highly dependent on divalent cations.[20] This is demonstrated by the observation that EDTA, which chelates such metal ions, renders ADAMTS13 completely inactive. A major reason for this is the removal of the active site Zn^{2+} ion. The coordination of a Zn^{2+} ion in the active site is essential for hydrolysis of the target peptide bond.[6] Like all ADAMTS family members, ADAMTS13 contains a characteristic active site motif in the metalloprotease domain that consists of 3 histidine residues that coordinate the catalytic Zn^{2+} ion. This sequence (HEXXHXXGXXHD) is highly conserved among all family members.[6]

In addition to Zn^{2+}, Ca^{2+} is also critical for the proteolysis of VWF by ADAMTS13.[20,23] A potential Ca^{2+}-binding site in the ADAMTS13 metalloprotease domain has been predicted, based on its homology with adamalysin II.[6,24] In this model of ADAMTS13, a single Ca^{2+} ion is proposed to be coordinated by Glu83, Asp173, Cys281, and Asp284 in the metalloprotease domain. However, although its importance may have been assumed, the functionality of this site has yet to be demonstrated. The exact contribution of Ca^{2+} to ADAMTS13 function has not been fully elucidated. Early studies provided some insight into the role of divalent cations in

Submitted March 11, 2008; accepted October 23, 2008. Prepublished online as *Blood* First Edition paper, December 1, 2008; DOI 10.1182/blood-2008-03-144683.

The publication costs of this article were defrayed in part by page charge payment. Therefore, and solely to indicate this fact, this article is hereby marked "advertisement" in accordance with 18 USC section 1734.

ADAMTS13 function. However, there also exist conflicting data: Tsai suggested that possibly only trace amounts of Ca^{2+} were sufficient for full ADAMTS13 activity.[20] Furlan et al suggested that whereas 10 mM Ca^{2+} or Sr^{2+} appreciably activated ADAMTS13, 10 mM Ba^{2+} maximally activated the enzyme.[21] This latter contention suggested that ADAMTS13 might be unique among metalloproteases in its preference for Ba^{2+} over Ca^{2+}. Perutelli et al reported efficient cleavage of the recombinant VWF A2 domain by ADAMTS13 without the addition of metal ions.[25] Anderson et al carried out the first systematic experimental investigation of the role of Ca^{2+} in ADAMTS13 function.[26] In that study, the authors reported an overall $K_{D(app)}$ of 4.8 μM (± 3.0 μM) for the Ca^{2+} ion dependence of ADAMTS13 function using multimeric VWF as a substrate in the presence of denaturants. The authors also used a fluorescent peptide substrate, FRET-VWF73 (a short recombinant VWF A2 domain fragment[27]), to study ADAMTS13 metalloprotease metal ion dependence. Their results demonstrated that ADAMTS13 activity was undetectable in the absence of both Zn^{2+} and Ca^{2+} ions, and that ADAMTS13 was markedly enhanced by Ca^{2+} ions. A $K_{D(app)}$ of approximately 60 μM for Ca^{2+} for the proteolysis of FRET-VWF73 by ADAMTS13 was reported. To endeavor to rationalize the discrepancies between different published reports, and to more fully characterize the functional Ca^{2+}-binding site(s) in ADAMTS13, we have examined the molecular basis of the Ca^{2+} dependence of ADAMTS13 activity. In this report, we provide evidence for the presence and location of a high-affinity functional Ca^{2+}-binding site in the ADAMTS13 metalloprotease domain.

Methods

Expression and purification of recombinant ADAMTS13, VWF, and VWF115

Recombinant purified human wild-type ADAMTS13 with a C-terminal Myc/His tag expressed in HEK293 cells was prepared and purified as previously described.[28-30] Mutagenesis of potential Ca^{2+}-binding residues was performed using the Quikchange site-directed mutagenesis kit (Stratagene, La Jolla, CA) according to the manufacturer's instructions. All vectors were verified by sequencing. Wild-type ADAMTS13 and its mutants were also expressed transiently in HEK293T cells using linear polyethylenimine (Polysciences, Warrington, PA) for transfection. Prior to use, both fully purified ADAMTS13 and transiently expressed ADAMTS13 in conditioned media were extensively dialyzed in 20 mM Tris (pH 7.8) using double deionized water (to ensure the absence of trace concentrations of any divalent cations). The ADAMTS13 concentration was determined using a specific in-house ADAMTS13 enzyme-linked immunosorbent assay (ELISA), as previously described.[17] The VWF A2 domain fragment, VWF115 (spanning VWF residues 1554-1668) was expressed, purified, and quantified as previously described for use as a specific ADAMTS13 metalloprotease domain substrate.[29] Full-length VWF was purified from plasma and quantified as previously described.[31]

ADAMTS13 activity assays

For time-course analysis of VWF115 proteolysis, 20 nM purified recombinant ADAMTS13 or 1 nM of expressed ADAMTS13 in conditioned media, both in 20 mM Tris-HCl (pH 7.8), 150 mM NaCl, and 0 to 8 mM $CaCl_2$ (as indicated) were preincubated at 37°C for 1 hour without VWF115 (unless otherwise stated). Thereafter, 1.6 μM VWF115 was added to start the reaction followed by incubation at 37°C. At different time points, 60 μL subsamples were removed, and reactions were stopped with 5 μL 0.5M EDTA. VWF115 proteolysis was quantified by high-performance liquid chromatography (HPLC) as previously described.[29] For investigation of metal ion dependence, reactions were set up as above, except ADAMTS13 in dialyzed conditioned media was preincubated for 1 hour at 37°C in 20 mM Tris-HCl (pH 7.8), 150 mM NaCl, and 10 mM metal ion ($CaCl_2$, $BaCl_2$, $MgCl_2$, $NiSO_4$, $MnCl_2$, or $CuSO_4$). The specificity constant, k_{cat}/K_m, of wild-type ADAMTS13 and mutant with D187A (at 5 mM Ca^{2+}) were also determined from time-course experiments with the substrate concentration below 1.0 μM, as described.[29] Michaelis-Menten plots were then used to determine individual K_m and k_{cat} values.[29]

To determine the Ca^{2+} dependence of ADAMTS13, the $K_{D(app)}$ (ie, the cation concentration required for a half maximal response [$V_{max}/2$]) was derived. For this, activity assays were set up as above using a range of Ca^{2+} concentrations (0-8 mM). Thereafter, early time points (0-10 minutes) were taken so that the proteolysis reactions were in the linear part of the time-course curve (ie, less than 15% VWF115 proteolysis). HPLC was used to quantify VWF115 cleavage, from which the initial rate of substrate proteolysis was determined. Data were fitted to parabolic plots, and the $K_{D(app)}$ for Ca^{2+} was determined by Graph Pad Prism 4 software (GraphPad, San Diego, CA) using the following equation: $Y = (V_{max} \times [Ca^{2+}]/(K_{D(app)} + [Ca^{2+}]))$, where Y is the initial rate of VWF115 proteolysis.

The Zn^{2+} dependence ($K_{D(app)}$) of ADAMTS13 was determined as in the equation except that ADAMTS13 was pretreated with EDTA and then extensively dialyzed and equilibrated into 20 mM Tris (pH 7.8) and 150 mM NaCl. This was then preincubated with 5 mM $CaCl_2$ prior to adding VWF115 in the presence of a range of Zn^{2+} concentrations (0-100 μM). After 5 to 10 minutes, reactions were stopped, and the initial rates of VWF115 proteolysis were determined before derivation of the V_{max} and $K_{D(app)}$, as described.

To ensure that our expressed ADAMTS13 was fully bound to Zn^{2+}, samples were treated with 15 mM EDTA for 30 minutes, dialyzed in 5 L 20 mM Tris-HCl (pH 7.8) for 4 hours, dialyzed again in 5 L 20 mM Tris-HCl with 500 μM $ZnCl_2$ for 4 hours, and finally equilibrated in 5 L 20 mM Tris-HCl and 150 mM NaCl for 4 hours. The initial rate of VWF115 cleavage was compared with ADAMTS13 that had not been treated with EDTA. Time-course reactions demonstrated that the initial rate for ADAMTS13 treated with EDTA was 0.23 nMs^{-1} compared with 0.25 nMs^{-1} for ADAMTS13 not subjected to EDTA and cation resupplementation. The V_{max} was also restored to its previous level by this protocol. These experiments demonstrated that resupplementation of divalent cations reversed the effect of EDTA. They also indicate that ADAMTS13 freshly expressed into conditioned media already contains Zn^{2+} in the active site. Therefore, in all assays (except those examining Zn^{2+} dependence) it was assumed that after dialysis the ADAMTS13 remained fully coordinated to Zn^{2+} but that all bound Ca^{2+} had been removed at the start of the experiment.

Purified plasma-derived VWF was also used as a substrate for ADAMTS13, using a previously reported activity assay.[26] For this, VWF was incubated with 1.5 M guanidine-HCl at 37°C for 1 hour. The denatured VWF was then diluted at least 10-fold to a final concentration of 80 nM into 150 mM NaCl, 20 mM Tris-HCl, and 5 mM $CaCl_2$ buffer, in which 5 nM ADAMTS13 had been preincubated for 60 minutes. The reaction was incubated at 37°C for 1 hour before quenching with 10 μL 0.5 M EDTA. The cleavage products were detected by multimer gel analysis and collagen-binding assay as previously described.[31-33]

Molecular modeling of ADAMTS13 metalloprotease domain

ADAMTS13 metalloprotease domain was modeled using its sequence homology to adamalysin II and the coordination for the crystal structure of this domain[24] (protein database file name 1IAG) using the SWISS-MODEL server.[34] Models were manipulated using Pymol software (Delano Scientific, Palo Alto, CA). Areas of dense surface negative charge were sought, and amino acids were identified that may comprise putative Ca^{2+} binding sites.

ADAMTS13 UV absorbance

To measure Ca^{2+}-dependent conformational changes in ADAMTS13, the absorbance at 280 nm UV light (Abs_{280}) by fully purified wild-type ADAMTS13 or ADAMTS13 E83A, D173A, and D187A mutants was measured using a UV-1601 spectrophotometer (Shimadzu, Kyoto, Japan). For this, 1 μM ADAMTS13 in 20 mM Tris-HCl (pH 7.8) was incubated with varying concentrations of $CaCl_2$ (0-8 mM) in the presence or absence of 150 mM NaCl. Abs_{280} was measured every minute for 60 minutes. Data

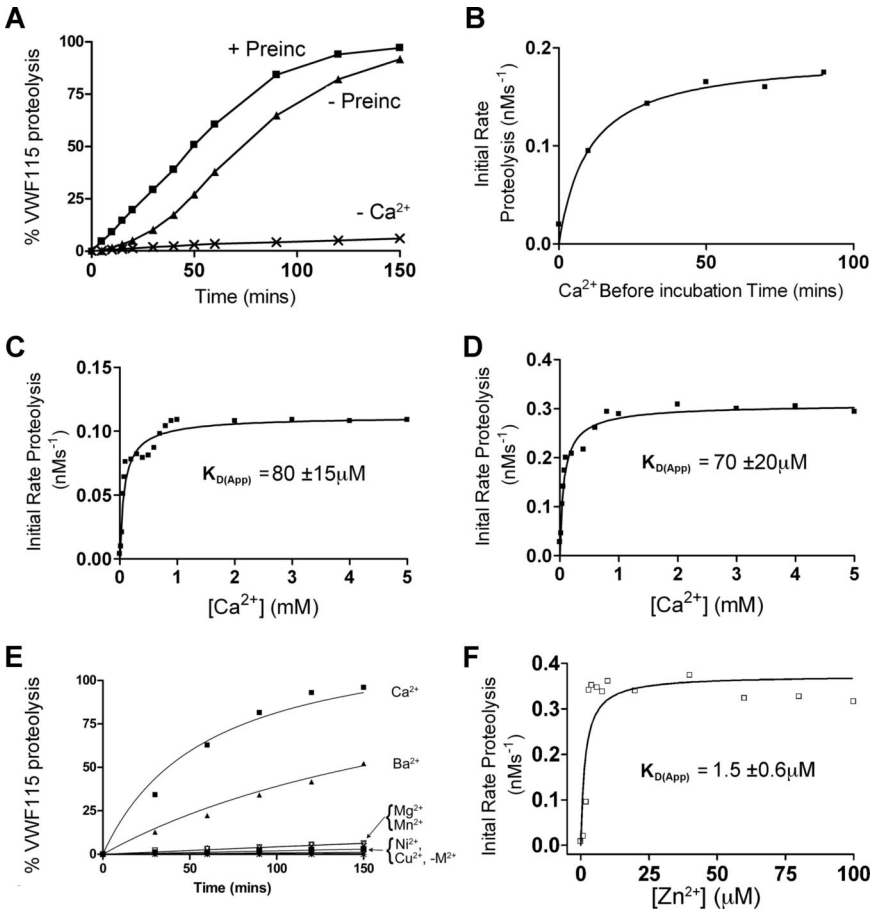

Figure 1. Ca^{2+} dependence of the VWF115 proteolysis by ADAMTS13. (A) 20 nM purified ADAMTS13 in 150 mM NaCl, 20 mM Tris-HCl (pH 7.8) was preincubated with 5 mM $CaCl_2$ for 60 minutes (+ Preinc), 0 minutes (−Preinc), or in the absence of $CaCl_2$ (−Ca^{2+}) before addition of 1.6 μM VWF115 substrate. Reactions were incubated at 37°C and stopped with EDTA, and VWF115 cleavage was quantified by HPLC. (B) The reaction conditions were as in panel A, but initial rates of substrate proteolysis by fully purified ADAMTS13 were determined as a function of preincubation time with 5 mM $CaCl_2$. (C) Reactions were set up again as in panel A, except that the concentration of $CaCl_2$ was varied and the $K_{D(app)}$ (± SD; n = 4) was derived for purified ADAMTS13. (D) 1 nM of ADAMTS13 in dialyzed conditioned medium was used under identical conditions to that used in panel C, and the $K_{D(app)}$ (± SD; n = 4) was again derived. (E) 1 nM of ADAMTS13 in dialyzed conditioned medium was studied as in panel A, except that preincubation was performed in the presence of 10 mM (final concentration) of $CaCl_2$, $BaCl_2$, $MgCl_2$, $NiSO_4$, $MnCl_2$, or $CuSO_4$. (F) 1 nM ADAMTS13 was pretreated with 15 mM EDTA to remove the Zn^{2+} ions, dialyzed and equilibrated in 150 mM NaCl, 20 mM Tris-HCl (pH 7.8), 5 mM $CaCl_2$, and varying concentrations of $ZnCl_2$ between 0 and 100 μM for 60 minutes at 37°C before addition of 1.6 μM VWF115 substrate. Reactions were stopped with EDTA after 10 minutes and proteolysis analyzed by HPLC, from which a $K_{D(app)}$ for Zn^{2+} of 1.5 μM (± 0.6 μM) was derived.

were fitted to a sigmoidal dose response curve using Prism software (GraphPad), from which the half maximal response (EC_{50}) was determined.

Results

Ca^{2+} dependence of ADAMTS13-mediated proteolysis of VWF115

To first assess the Ca^{2+} dependency of ADAMTS13, time-course experiments were conducted. Initial experiments (Figure 1A-C) used fully purified ADAMTS13. Under the assay conditions used, almost no proteolysis of VWF115 substrate occurred using purified ADAMTS13 unless Ca^{2+} ions were added to the reaction buffer (Figure 1A). This showed that purification and dialysis of ADAMTS13 was able to remove essentially all functional Ca^{2+}, but it did not remove the active site-bound Zn^{2+} (known to be essential for any activity), and that any trace divalent metal ions in the buffers used were unable to appreciably activate the protease. In time-course reactions in the presence of Ca^{2+} set up without prior preincubation with this cation before the addition of VWF115, we detected a "lag phase" in VWF115 proteolysis, whereas this was not evident when ADAMTS13 was preincubated with Ca^{2+} for 1 hour prior to the addition of VWF115 (Figure 1A). To confirm this finding, and to determine the optimal Ca^{2+} preincubation time required to "activate" ADAMTS13, the initial rate of VWF115 proteolysis was titrated as a function of Ca^{2+} preincubation time. These results confirmed that Ca^{2+} ions do not fully activate ADAMTS13 immediately. Indeed, the full activation of ADAMTS13 by Ca^{2+} took 40 to 50 minutes, even at high Ca^{2+} concentrations (5 mM) much higher then the previously reported $K_{D(app)}$,[26] suggesting that complete association of this cation takes place comparatively slowly (Figure 1B).

To investigate further the Ca^{2+} dependence of purified ADAMTS13, the influence of Ca^{2+} concentration upon the initial rate of VWF115 proteolysis was determined. Following 1 hour of preincubation of ADAMTS13 with varying concentrations of Ca^{2+} (0-5 mM), VWF115 was added and reactions were stopped after 5 or 10 minutes. To ensure accurate kinetic analyses, initial rates of VWF115 proteolysis were determined from samples with less than 15% substrate cleavage. Using purified ADAMTS13, a mean (± SD; n = 4) $K_{D(app)}$ for Ca^{2+} of 80 μM (± 15 μM) was determined (Figure 1C). This value is in good agreement with the data reported by Anderson et al (60 ± 25 μM) using FRET-VWF73.[26] Using ADAMTS13 that had been expressed in conditioned medium, concentrated and then thoroughly dialyzed, a very similar value of 70 μM (± 20 μM) was obtained (Figure 1D). It was noted, however, that despite the similarity in these $K_{D(app)}$ values, the maximal activity (V_{max}) of purified ADAMTS13 was appreciably lower than that of ADAMTS13 in dialyzed conditioned media (compare Figure 1C and 1D). Moreover, lower ADAMTS13 antigenic concentrations in conditioned media (1 nM compared with 20 nM) were needed to proteolyse the substrate at a similar rate. This reduced V_{max} was attributed to loss of activity during purification (indeed, determination of k_{cat} and K_m values of ADAMTS13 in conditioned media containing Ca^{2+} produced estimates of k_{cat}/K_m that were approximately 10-fold increased compared with values we have published using purified ADAMTS13[29]; see below). This reduction in V_{max} was a potential

obstacle for the comparison of responses of fully purified mutants (see below) to Ca^{2+}. Consequently, the Ca^{2+} induced functional responses of wild-type and mutant ADAMTS13 against substrate (VWF115 and full-length VWF) proteolysis were subsequently compared using extensively dialyzed conditioned media samples rather than purified material.

The activity of ADAMTS13 in the presence of different metal ions was also determined. This demonstrated that Ca^{2+} is the most potent activating divalent cation out of 6 (Ca^{2+}, Ba^{2+}, Mg^{2+}, Mn^{2+}, Ni^{2+}, and Cu^{2+}) tested (Figure 1E). Ba^{2+} was the only other metal ion to have any appreciable effect on ADAMTS13 activity, which is compatible with prior reports in the literature.[26] It has been suggested that Ca^{2+} and Zn^{2+} act synergistically with respect to ADAMTS13 activity.[26] To explore the Zn^{2+} dependence of activity, ADAMTS13 in selected experiments was pretreated with EDTA to remove all cations as described in "Methods," preincubated with 5 mM Ca^{2+}, then titrated with Zn^{2+}. Figure 1F demonstrates an absolute requirement of Zn^{2+} for activity. Fitting the results of Figure 1F to the equation in "Methods" revealed a $K_{d(app)}$ of 1.5 μM (± 0.6 μM).

Ca^{2+} induces a conformational change in ADAMTS13, but only under low-ionic-strength conditions

To examine the possibility of conformational changes induced by Ca^{2+} ions, the change in Abs_{280} of purified ADAMTS13 was examined over time in the presence of 5 mM Ca^{2+}. We detected a large change in Abs_{280} of ADAMTS13 in response to Ca^{2+}, but only in the absence of NaCl. At 0 minutes, ADAMTS13 Abs_{280} was the same in all samples. However, in the presence of Ca^{2+}, the Abs_{280} had increased markedly over the course of 1 hour, whereas it remained unchanged in the absence of Ca^{2+} or in the presence of 150 mM NaCl (Figure 2A). These data are indicative of a conformational change in response to Ca^{2+} binding that alters the relative exposure/orientation of surface residues such as Trp, Tyr, and Phe. Further analyses revealed that this change in absorbance occurs slowly, with the Abs_{280} increase only detectably starting after an approximately 20-minute lag phase, and reaching completion after approximately 50 minutes (Figure 2B). Using a 1-hour preincubation time, the Ca^{2+} concentration dependence of this change was titrated (Figure 2C), revealing an EC_{50} value of 880 μM, which is appreciably higher than the kinetically derived $K_{D(app)}$value of 70 to 80 μM for VWF115 proteolysis (Figure 1C,D). The change in Abs_{280} induced by Ca^{2+} could conceivably be attributed to aggregation of the sample. This possibility was discounted by electrophoresis of ADAMTS13 on a native PAGE gel in the presence and absence of NaCl and $CaCl_2$, which showed that ADAMTS13 migrated as a distinct band (data not shown). These observations, together with the need to omit NaCl to observe the conformational change, suggests that the influence of Ca^{2+} observed in Figure 2 is mediated through a distinct site to that determining the high-affinity proteolysis response observed in Figure 1.

Modeling of ADAMTS13 metalloprotease domain

As there are no structural data on ADAMTS13 to date, modeling of the ADAMTS13 metalloprotease domain using the known adamalysin II structure was done to search for putative Ca^{2+}-binding sites. From this, the Ca^{2+}-binding site predicted by Zheng et al[6] is apparent (Figure 3A). This putative Ca^{2+}-binding site involves Glu83, Asp173, Cys281, and Asp284 in ADAMTS13, and is called Site 1. Glu83 and Asp173 are perfectly conserved. Cys281 is predicted to coordinate Ca^{2+} through its carbon backbone rather than the amino acid R-group. This site is on the opposite side of the

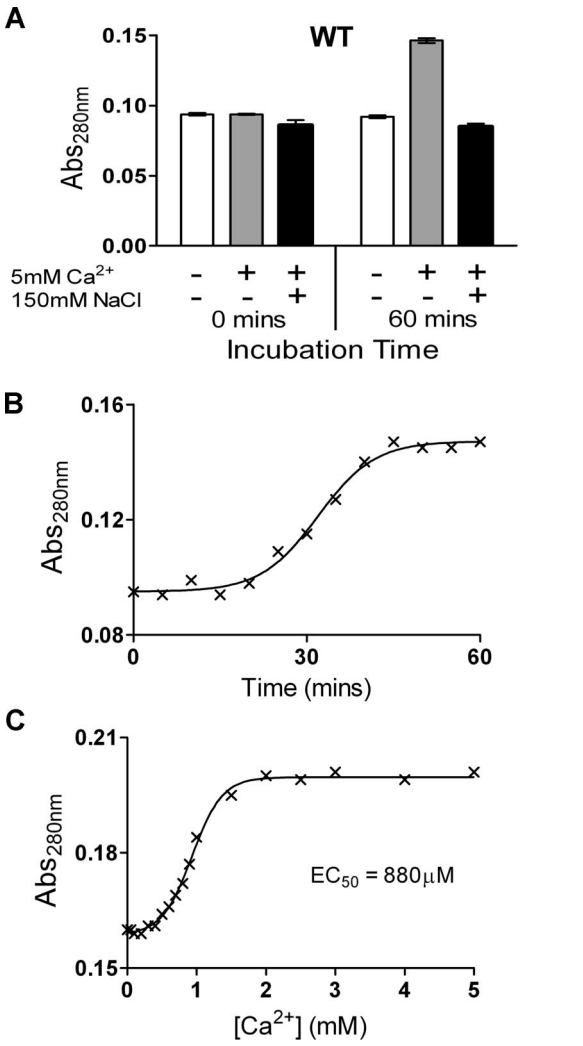

Figure 2. Ca^{2+} causes a change in absorbance of ADAMTS13, but only in low-ionic-strength conditions. (A) The Abs_{280} (± SD) of 1 μM of purified ADAMTS13 in 20 mM Tris-HCl (pH 7.8) with or without 10 mM $CaCl_2$, and with or without 150 mM NaCl, was measured at 0 minutes and 60 minutes after the addition of $CaCl_2$ and/or NaCl. (B) Change in Abs_{280} of 1 μM ADAMTS13 in 20 mM Tris-HCl (pH 7.8) and 10 mM $CaCl_2$ over 60 minutes. (C) Change in Abs_{280} of 1 μM ADAMTS13 in 20 mM Tris-HCl (pH 7.8) preincubated for 1 hour with 0 to 5 mM $CaCl_2$. From these data, the EC_{50} was derived.

metalloprotease domain to the active site and is highly conserved in matrix metalloproteinases (MMPs).

Two further potential Ca^{2+}-binding sites (called Site 2 and Site 3) were also identified based on the presence of clusters of Asn, Asp, and Glu residues (Figure 3B,C). Site 2 is located relatively close to Site 1, and involves residues in proximity on a contiguous sequence potentially involving a combination of Asn162, Glu164, Asp165, Asp166, and Asp168. Site 3 is located on the other side of the metalloprotease domain to Site 1 and Site 2, adjacent to the active site cleft involving Asp187 and Glu212, and either Asp182 or Glu184 (Figure 3C). Glu184 and Asp187 are not conserved, whereas Asp182 and Glu212 are well conserved among the ADAMTS family.

The Ca^{2+}-induced change in absorbance of ADAMTS13 under low-ionic-strength conditions is lost by mutation of Site 1

To investigate the functional response of Site 1 to Ca^{2+}, 2 ADAMTS13 single-point mutants, E83A and D173A, were

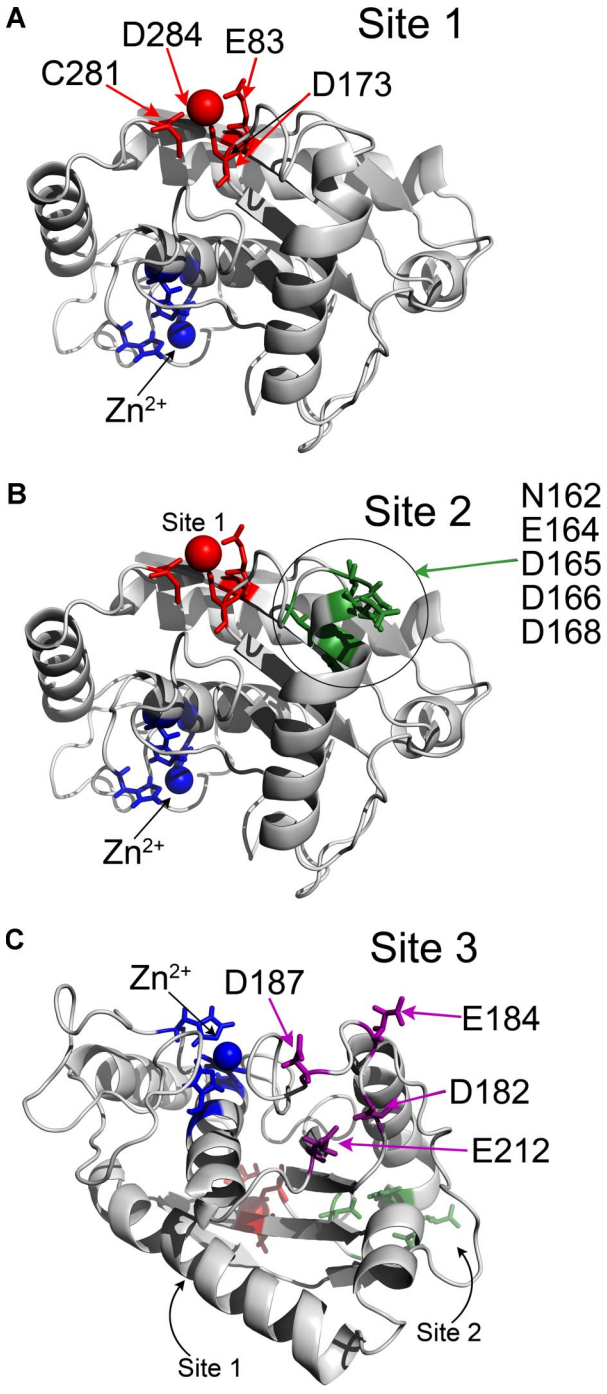

Figure 3. Identification of putative Ca^{2+}-binding sites in ADAMTS13 metalloprotease domain by homology modeling. (A-C) The ADAMTS13 metalloprotease domain was homology-modeled using the crystal structure of adamalysin II (1IAG). Structures are depicted in cartoon format. Zn^{2+} ion and 3 active-site His residues are shown in blue. (A) Site 1 predicted to involve E83, D173, C281, and D284 is shown in red. Ca^{2+} ion also present in adamalysin II crystal structure in a homologous site is shown as a red sphere. (B) Putative Site 2 is in proximity to Site 1 (shown in red) and may involve residues N162, E164, D165, D166, and D168, which are highlighted in green. (C) Putative Site 3 is located on the opposite side of the metalloprotease domain to Site 1 and Site 2 (shown in red and green, respectively) and lies adjacent to the active-site cleft. Site 3 may involve residues D182, E184, D187, and E212, which are shown in purple.

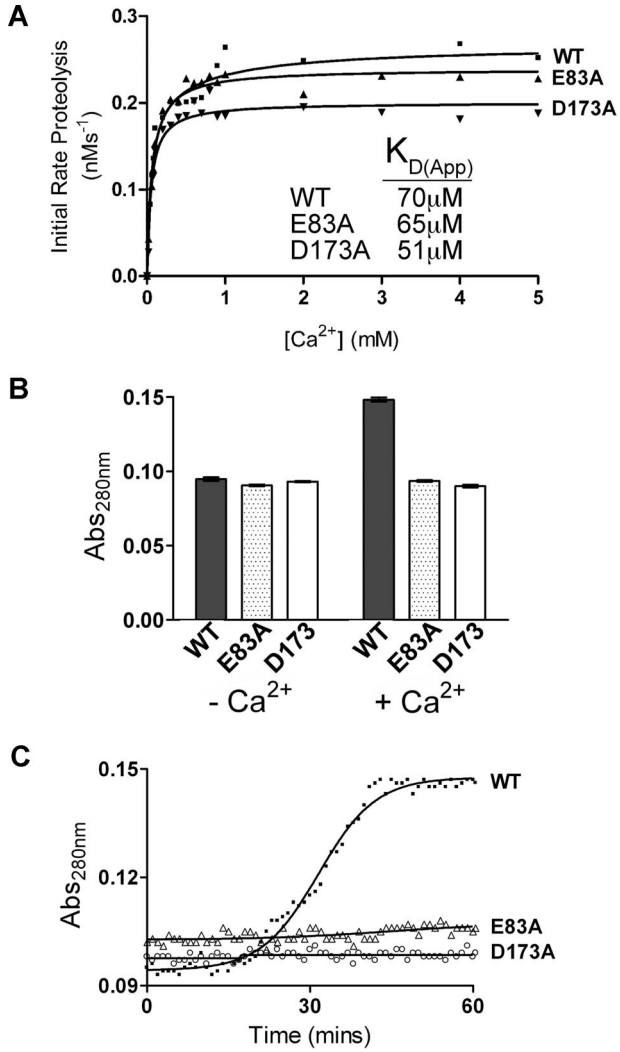

Figure 4. Mutagenesis of Site 1 abolishes the Ca^{2+}-induced conformational change in ADAMTS13 observed under low-ionic-strength conditions. Analysis of putative Site 1 residue mutants. (A) 1 nM ADAMTS13 wild-type, E83A, or D173A in 150 mM NaCl and 20 mM Tris-HCl (pH 7.8) was preincubated with 0 to 5 mM $CaCl_2$ for 60 minutes at 37°C before addition of 1.6 μM VWF115 substrate. After 10 minutes, reactions were stopped with EDTA, and VWF115 cleavage was quantified by HPLC, from which initial rates of substrate proteolysis were determined. Initial rates are plotted as a function of Ca^{2+} concentration, from which the $K_{D(app)}$ was derived. (B) The Abs_{280} (± SD) of 1 μM purified ADAMTS13 (■; WT), E83A (▨), or D173A (□) in 20 mM Tris-HCl (pH 7.8) plus or minus 10 mM $CaCl_2$ was measured at 0 minutes and 60 minutes after the addition of $CaCl_2$. (C) Change in Abs_{280} of 1 μM ADAMTS13 (WT), E83A, and D173A in 20 mM Tris-HCl (pH 7.8) and 10 mM $CaCl_2$ over 60 minutes.

generated to disrupt Ca^{2+} binding to this site (Figure 3A). These mutants were then tested for functional Ca^{2+} dependence using the same assays used previously to characterize wild-type ADAMTS13. The E83A and D173A mutants showed an overall $K_{D(app)}$ for Ca^{2+} of 65 μM and 51 μM, respectively (Figure 4A), which is very similar to the data derived for wild-type ADAMTS13. In the absence of NaCl, however, neither of these mutants exhibited any change in Abs_{280} in the presence or absence of 5 mM Ca^{2+}, even after 1 hour (Figure 4B,C). Even when Ca^{2+} was increased to 8 mM, we detected no change in Abs_{280} for either of these mutants (data not shown). These data revealed that the Ca^{2+}-induced absorbance change detected under low-ionic-strength conditions in wild-type ADAMTS13 had been abolished by either of the E83A or D173A substitutions and was therefore mediated by Site 1. They also suggest that whereas these residues most likely bind Ca^{2+}, this does not appreciably influence substrate cleavage under normal ionic conditions.

Site 2 is not a functional Ca^{2+}-binding site

From our molecular modeling, the putative Ca^{2+}-binding site called Site 2 (Figure 3B) could potentially involve several residues

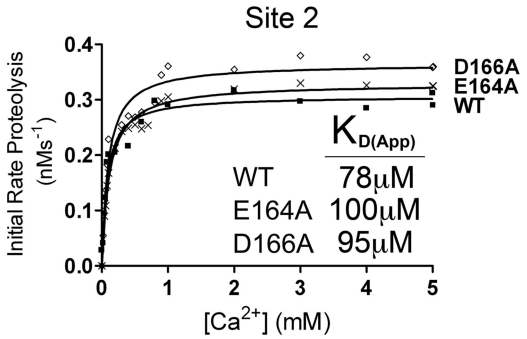

Figure 5. Putative Site 2 is not a high-affinity functional binding site. Analysis of putative Site 2 mutants. 1 nM transiently expressed ADAMTS13 (WT) or E164A or D166A Site 2 mutant in 150 mM NaCl and 20 mM Tris-HCl (pH 7.8) were preincubated with 0 to 8 mM $CaCl_2$ for 60 minutes at 37°C before addition of 1.6 μM VWF115 substrate. After 10 minutes, reactions were stopped with EDTA, and VWF115 cleavage was quantified by HPLC, from which initial rates of substrate proteolysis were determined. Initial rates are plotted as a function of Ca^{2+} concentration, from which the $K_{D(app)}$ was determined.

in a short sequence spanning residues 162 to 168 of the metalloprotease domain. To determine whether Site 2 corresponded to the high-affinity functional Ca^{2+}-binding site, E164A and D166A mutants were generated and the Ca^{2+} dependence of VWF115 proteolysis was analyzed (Figure 5). From the initial rate of VWF115 cleavage data, we derived $K_{D(app)}$ values that were very similar to those derived for wild-type ADAMTS13 (Figure 5). The lack of any functional deficit in either the E164A or D166A mutants strongly suggested that Site 2 is not a functionally important Ca^{2+}-binding site.

Site 3 is the functional high-affinity Ca^{2+}-binding site and is essential for full ADAMTS13 activity

The putative Ca^{2+}-binding site, called Site 3, is predicted to involve residues Asp182 or Glu184, Asp187, and Glu212 (Figure 3C). We made E184A, D187A, and E212A substitutions because 2 of these residues are unique to ADAMTS13 (Glu184 and Asp187) among the ADAMTS family, and one is highly conserved (Glu212). Following generation of E184A, D187A, and E212A mutants, we measured the Ca^{2+} dependence of VWF115 cleavage. As before, wild-type ADAMTS13 showed a characteristic $K_{D(app)}$ for Ca^{2+} of 72 μM. The E184A mutant exhibited a V_{max} that was very similar to wild-type ADAMTS13 (Figure 6A). However, it was clear that it had reduced Ca^{2+} dependence, as observed by the shift of the curve to higher concentrations of Ca^{2+}. We derived a $K_{D(app)}$ value of 242 μM (as compared with the 72 μM derived for wild-type ADAMTS13). This suggested that the binding of Ca^{2+} to the high-affinity site had been compromised by this mutant rather than abolished. The data for D187A and E212A mutants were more

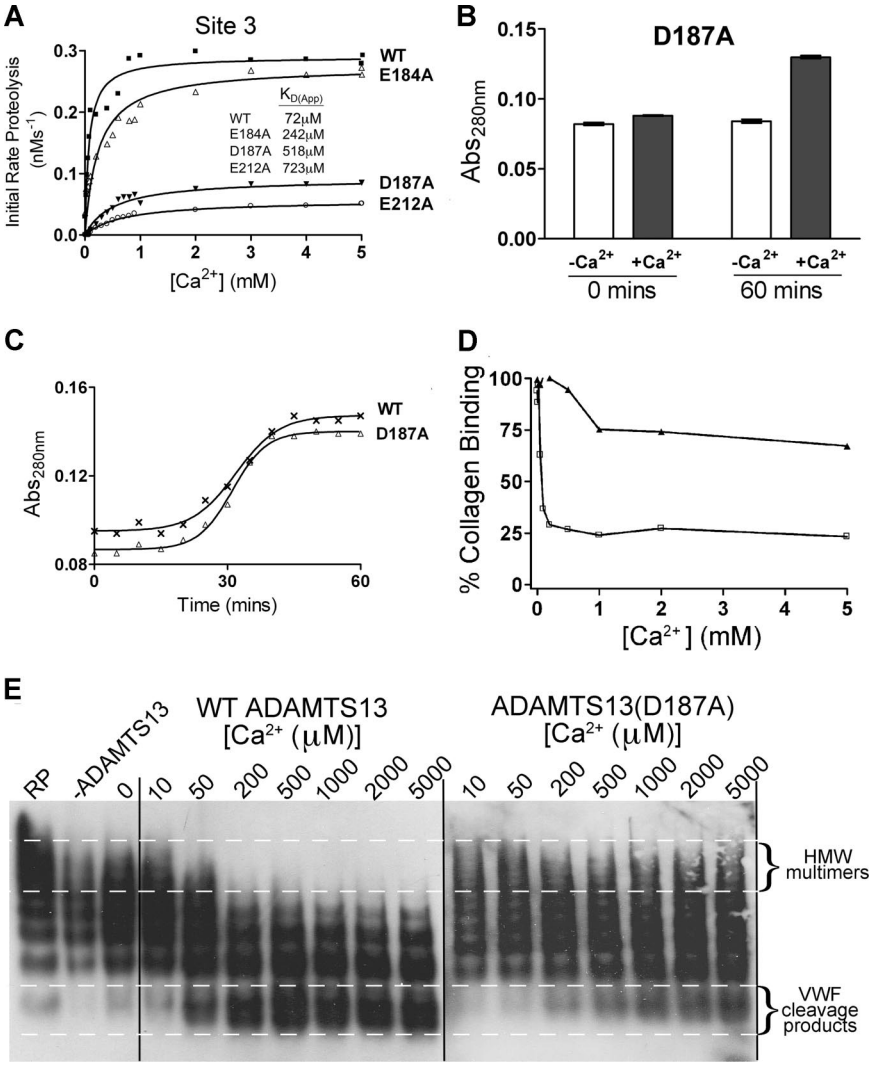

Figure 6. Site 3 is a high-affinity functional Ca^{2+}-binding site and is critical for ADAMTS13 activity. (A) Analysis of putative Site 3 mutants. 1 nM transiently expressed ADAMTS13 (WT), E184A, D187A, or E212A Site 3 mutants in 150 mM NaCl and 20 mM Tris-HCl (pH 7.8) were preincubated with 0 to 5 mM $CaCl_2$ for 60 minutes at 37°C before addition of 1.6 μM VWF115 substrate. After 10 minutes, reactions were stopped with EDTA and VWF115 cleavage was quantified by HPLC, from which initial rates of substrate proteolysis were determined. Initial rates are plotted as a function of Ca^{2+} concentration, from which the $K_{D(app)}$ was derived. (B) The Abs_{280} (± SD) of 1 μM purified ADAMTS13 D187A mutant in 20 mM Tris-HCl (pH 7.8) in the absence (□) or presence (■) of 10 mM $CaCl_2$ was measured at 0 minutes and 60 minutes after the addition of $CaCl_2$. (C) Change in Abs_{280} of 1 μM purified ADAMTS13 (WT) or D187A mutant in 20 mM Tris-HCl (pH 7.8) and 10 mM $CaCl_2$ over 60 minutes. (D,E) Plasma-derived purified full-length VWF was pretreated with 1.5 M guanidine-HCl to denature the protein and then added to a preincubating mixture of 5 nM wild-type or D187A mutant, 150 mM NaCl, 20 mM Tris-HCl (pH 7.8), and varying $CaCl_2$ concentrations between 0 and 5 mM. The reaction was incubated at 37°C for 60 minutes before quenching with EDTA. Samples were analyzed by collagen-binding assay to assess the ability of the remaining VWF in the sample to bind human collagen type III (D). Samples were also run on a 1.4% agarose gel with subsequent Western blotting to detect VWF multimeric composition (E).

Table 1. Kinetic analysis of wild-type ADAMTS13 and mutant D187A ADAMTS13 proteolysis of VWF115

ADAMTS13	Time course (n = 3), k_{cat}/K_m, $10^6\ M^{-1}s^{-1}$	Michaelis-Menten		
		K_m, μM	k_{cat}, s^{-1}	k_{cat}/K_m, $10^6\ M^{-1}s^{-1}$
Wild-type	1.24 ± 0.10	1.29	1.31	1.02
D187A	0.10 ± 0.02	4.32	0.31	0.07

dramatic (Figure 6A). Both mutants showed appreciably reduced V_{max} (3- and 4-fold, respectively). Furthermore, for each mutant, the $K_{D(app)}$ was appreciably altered, at 520 μM for D187A, and 720 μM for E212A (Figure 6A). This strongly suggests that the binding of Ca^{2+} to the high-affinity site has been greatly attenuated or abolished in these mutants.

To examine the contribution of this high-affinity Ca^{2+}-binding site to the proposed conformational change induced in ADAMTS13 under low ionic conditions in the presence of Ca^{2+}, absorbance studies were performed with the D187A mutant under low-ionic-strength conditions, as before. The conformational change in response to incubation with Ca^{2+} remained the same as wild-type ADAMTS13 (Figure 6B,C), consistent with this effect being mediated by the low-affinity Site 1. This suggests that the 2 potential Ca^{2+}-binding sites have independent effects.

To investigate possible mechanisms by which Ca^{2+} occupancy of Site 3 influences ADAMTS13 proteolysis of VWF115, kinetic investigations were carried out using wild-type and mutant ADAMTS13 with VWF115 in the presence of 5 mM Ca^{2+}. Time-course analysis (n = 3) carried out with 0.85 nM wild-type ADAMTS13 and VWF115 (< 1 μM) revealed k_{cat}/K_m values of 1.24 (± 0.10) × $10^6\ M^{-1}s^{-1}$, whereas this was reduced to 0.10 (± 0.02) × $10^6\ M^{-1}s^{-1}$ for the D187A mutant (Table 1). Michaelis-Menten constants, K_m, and the turnover number, k_{cat}, were determined by titration with increasing and saturating amounts of substrate (Table 1). For wild-type ADAMTS13, the K_m for VWF115 was found to be 1.29 μM and k_{cat} to be 1.31 s^{-1}. The corresponding values for the D187A mutant were 4.32 μM and 0.31 s^{-1}.

The D187A mutant was further investigated in full-length VWF assays to determine the influence of this mutation, and hence this site, with the physiologic substrate. Plasma-purified VWF (pretreated with guanidine-HCl) was incubated with both wild-type ADAMTS13 and D187A mutant preincubated with varying Ca^{2+} concentrations (0-5 mM). Figure 6D shows the analysis of these samples using a collagen-binding assay. VWF after incubation with wild-type ADAMTS13 had greatly reduced collagen-binding function when compared with VWF treated with D187A mutant. The VWF cleavage products were also analyzed on a multimer gel (Figure 6E). This clearly shows a difference between wild-type ADAMTS13 and D187A mutant in both the rate of proteolysis (as shown by a greater number of high-molecular-weight bands after time with the mutant compared with wild-type ADAMTS13) and also the Ca^{2+} dependence (with low-molecular-weight bands appearing at much higher Ca^{2+} concentrations in the mutant (500-1000 μM) than with wild-type ADAMTS13 (50-200 μM).

Discussion

In the present study, we aimed to characterize the Ca^{2+} dependence of the functional activity of ADAMTS13. Here, we report for the first time that Ca^{2+} ions do not fully activate ADAMTS13 immediately upon addition, with full activation occurring only after 40 minutes of incubation with Ca^{2+} ions. This has obvious implications for the design of functional assays for ADAMTS13, which should allow time for equilibration of the protease and Ca^{2+} ions. We also demonstrate that Ca^{2+} and Zn^{2+} ions have independent roles in protease activity, with both ions absolutely required for expression of activity. The requirement for Zn^{2+} ions is no surprise in view of its known role in the ADAMTS family, forming an essential part of the active center. It is also known that Ca^{2+} is needed for optimum activity, but there have been disparate findings on its importance, and the mechanism for Ca^{2+}-induced activation has not been fully addressed before. The speculation in the literature about possible functional Ca^{2+}-binding sites in ADAMTS13[6,26] have not before been subjected to formal evaluation of their roles. The homology model of the ADAMTS13 metalloprotease domain, based on the crystal structure of adamalysin II, identified a putative Ca^{2+}-binding site (Site 1) in ADAMTS13 predicted to be coordinated by Glu83, Asp173, Cys281, and Asp284 (Figure 3A).[6] These residues are broadly conserved among ADAMTS family members and other metalloproteinase domains. For this reason, Ca^{2+} binding to this site may also be a common feature of ADAMTS proteins.[23] The present study found that a response (change in absorbance) to occupancy of this site by Ca^{2+} could be measured, but only under low-ionic-strength conditions. This response was attributed to a conformational change in the metalloprotease domain of ADAMTS13. Absorbance measurements of mutants of this potential site to which Ca^{2+} had been added under low-ionic-strength conditions showed no changes in Abs_{280} over time (Figure 4B,C), or with increasing ion concentration (data not shown), suggesting that the Ca^{2+}-dependent conformational change had been ablated in these mutants. Together, these results strongly suggest that Glu83 and Asp173 (in conjunction with Cys281 and Asp284) comprise a potential low-affinity Ca^{2+}-binding site in ADAMTS13. Gerhardt et al identified a double Ca^{2+} site in ADAMTS1[35] in the region corresponding to the low-affinity Site 1 in ADAMTS13, which is also present in ADAMTS4 and ADAMTS5.[36] The double Ca^{2+}-binding site appears to be a unique feature of ADAMTS family metalloprotease domains, although whether all members of this family bind 2 Ca^{2+} ions at this site remains to be established. It is thought that in ADAMTS1, this double site may help stabilize/mediate folding and reorientation of a polypeptide loop connecting the metalloprotease and disintegrin-like domains. This appears to position the disintegrin-like domain close to the active site at the other end of the catalytic domain.[35] This is also thought to be the case in ADAMTS4 and 5.[36] Conceivably, such a conformational change may contribute to the Ca^{2+}-dependent Abs_{280} changes seen with ADAMTS13 under low ionic conditions. This process might involve repositioning of the more C-terminal domains to align with the active site of the metalloprotease. For this reason, it has been suggested that the disintegrin-like domain in ADAMTS1 could represent an auxiliary substrate binding surface and so be directly involved in substrate recognition.[35] Although the large conformational changes observed in Figures 2, 4, and 6 are largely inhibited by NaCl, it remains to be determined whether more discrete changes still occur and might contribute to the multiple interactions required for ADAMTS13 function. It must be considered though that short substrate (VWF115) proteolysis is largely unaffected by this site, which is demonstrated by the essentially unaltered Ca^{2+} dependence of VWF115 proteolysis on mutagenesis of residues Glu83 and Asp173 (Figure 4A).

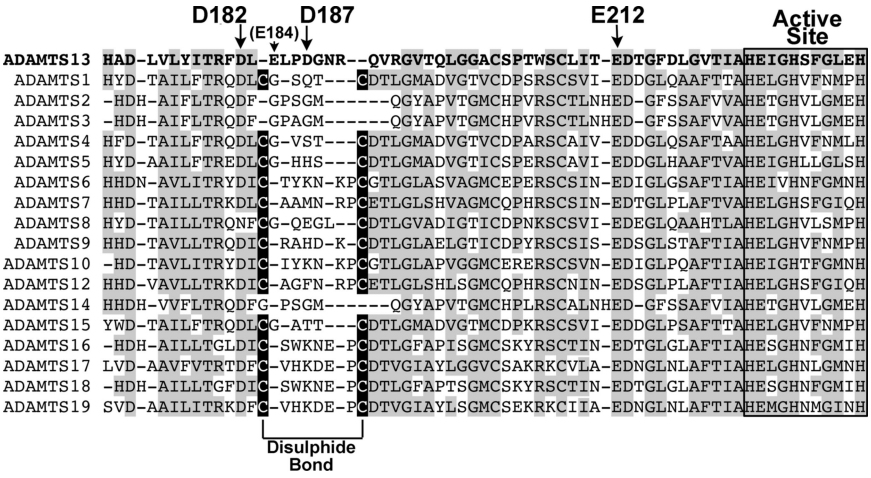

Figure 7. Alignment of ADAMTS13 Ca^{2+}-binding site with other ADAMTS family members. ADAMTS13 metalloprotease domain (residues 171-234) were aligned with corresponding regions of other ADAMTS family members. Regions of amino acid conservation are highlighted in gray. The active site amino acids are boxed/labeled. High-affinity Ca^{2+}-binding residues in ADAMTS13 are labeled with arrows. The Cys residues in all ADAMTS family members except ADAMTS2, 3, 13, and 14 that pair to form a disulphide bond are highlighted in black boxes.

The evidence for the presence and importance of a high-affinity functional binding site is compelling. Prior to the present study, despite data highlighting the importance of Ca^{2+} for ADAMTS13 function, there was no indication based on functional studies as to the location of a Ca^{2+}-binding site within the ADAMTS13 metalloprotease domain. Inspection of the homology model, together with sequence conservation between ADAMTS family members and MMPs, helped identify 2 candidate high-affinity sites; Site 2 predicted to involve residues Glu164 and Asp166 (in conjunction with one or more of Asn162, Asp165, and Asp168; Figure 3B), and Site 3 predicted to involve residues Asp187 and Glu212 in conjunction with Asp182 or Glu184 (Figure 3C). The suggestion of Site 3 was supported by comparison of the ADAMTS13 metalloprotease domain homology model with the crystal structure of MMP8,[37] from which clear similarities in this Ca^{2+}-binding site can be seen. The present study demonstrates that mutating Site 3 residues in ADAMTS13 to alanine attenuates high-affinity Ca^{2+}-induced functional activity (Figure 6A), strongly suggesting that they comprise the high-affinity Ca^{2+}-binding site. Interestingly, the D184A mutant did not alter the V_{max} of ADAMTS13 for VWF115 proteolysis, but it did increase the $K_{D(app)}$. For this reason, it appears that this mutation reduced the affinity for Ca^{2+} at this site, rather than abolished binding completely. This suggests that this residue does not have a major role in Ca^{2+} coordination, and that nearby Glu182 is more likely the residue that fulfills this function (Figure 7). Conversely, the D187A and E212A mutants exhibited both a markedly increased $K_{D(app)}$ and a reduced V_{max}. Together, these observations are suggestive of an appreciable or even a complete loss of Ca^{2+} binding to the high-affinity Site 3. This result is supported at least semiquantitatively by Figure 6D and 6E, which shows decreased activity of the D187A mutant compared with wild-type ADAMTS13 against full-length VWF. Despite the large influence of mutating this site on Ca^{2+} functional responses, ADAMTS13 still exhibited some residual concentration-dependent response to Ca^{2+} in reaction with VWF115. Whether the residual activity represents the function of another distinct functional Ca^{2+}-binding site remains to be determined. It is clear, though, that the majority of the effects that Ca^{2+} has upon ADAMTS13 cleavage of VWF115 is mediated through binding to this high-affinity site. Further support for a site-specific Ca^{2+} functional role was provided by mutation of Site 2 of ADAMTS13 (involving similarly charged residues, Glu164 and Asp166). These substitutions had no effect upon ADAMTS13 function or its Ca^{2+} dependence (Figure 5). The data presented in this manuscript also suggest that the high- and low-affinity sites respond to Ca^{2+} independently. For example, the Site 3 D187A mutant ADAMTS13 still exhibited Ca^{2+}-dependent changes in Abs_{280} over time under low ionic conditions (Figure 6B,C).

Inspection of the proposed high-affinity site of ADAMTS13 and comparison of the residues involved with the equivalent region in other ADAMTS family members reveals an interesting variation. In most of the other ADAMTS metalloproteases, there are 2 Cys residues that form an internal disulphide bond (Figure 7). It seems, therefore, that this loop adjacent to the active site may be held in a stable conformation by the disulphide bond that is present in most ADAMTS family members. In ADAMTS13, these Cys residues are not present. Consequently, in ADAMTS13 this loop may be held in a stable/active conformation by a Ca^{2+} ion, which provides a rationale for the functional importance of this site. This contention is corroborated by MMP8, in which the equivalent loop that (like ADAMTS13) also lacks a disulphide bond, and appears to be held in a stable conformation by a Ca^{2+} ion.[37]

During the preparation of this manuscript, 3 papers were published that describe the crystal structures of the metalloprotease domains of ADAMTS1,[35] ADAMTS4,[36] and ADAMTS5.[36,38] Those involving ADAMTS4 and ADAMTS5 report a Ca^{2+}-binding site in a similar position to Site 3 in ADAMTS13, although here, there is also a disulphide bond present. The disulphide bond will stabilize the loop, with a bound calcium ion perhaps also contributing.

Further kinetic analysis of the reaction between wild-type ADAMTS13 and VWF115, and D187A and VWF115 revealed a possible mechanism of action of this high-affinity Ca^{2+}-binding site. Time-course analysis carried out with wild-type ADAMTS13 and VWF115 revealed k_{cat}/K_m values of $1.24\,(\pm 0.10) \times 10^6\,M^{-1}s^{-1}$, whereas this was reduced to $0.10\,(\pm 0.02) \times 10^6\,M^{-1}s^{-1}$ for the D187A mutant (Table 1). For wild-type ADAMTS13, the K_m for VWF115 was found to be 1.29 μM and k_{cat} to be $1.31\,s^{-1}$. The corresponding values for the D187A mutant were 4.32 μM and $0.31\,s^{-1}$. The increase in K_m implies that the mutation of D187A affects the functional binding affinity between the substrate and the active site of the enzyme. The reduction in k_{cat} points to a reduction also in substrate turnover, while the 13-fold reduction in catalytic efficiency provides an overall measure of the decrease in proteolytic activity of the mutated enzyme. These results directly link the mutation of a residue in a Ca^{2+}-binding site to a reduction in functional substrate binding and activity, suggesting that Ca^{2+} in this site may normally serve to stabilize this loop region such that the substrate is optimally placed in the active site for efficient proteolysis. Intriguingly, in ADAMTS4 and ADAMTS5 there is no residue homologous to Asp187 in ADAMTS13,

while the homologous residue to Glu212 is present, as it is in all ADAMTS family members and most MMPs. Since it is evident that Asp187 is important to activity and calcium binding in ADAMTS13, this different coordination of Ca^{2+} may be necessary for the Ca^{2+} ion to stabilize the whole loop by itself, as there is no disulphide bond to aid in this function. If so, ADAMTS13 may be more dependent on Ca^{2+} for function than other ADAMTS metalloproteases.

Acknowledgments

This work was supported by British Heart Foundation grants RG/02/008 and FS/06/002 (to J.T.B.C., C.K.N.K.C., and D.A.L.), an unrestricted grant from Amgen, and the National Institute for Health Research (NIHR) Biomedical Research Center Funding.

Authorship

Contribution: M.D.G. performed experiments, analyzed results, and wrote the paper; C.K.N.K.C. performed experiments, analyzed results, and designed the research; R.d.G. performed experiments and analyzed results; A.S. performed experiments; J.T.B.C. designed the research, analyzed results, wrote the paper, and made the figures; and D.A.L. designed the research, analyzed results, and wrote the paper.

Conflict-of-interest disclosure: The authors declare no competing financial interests.

Correspondence: James T. B. Crawley, Department of Haematology, Imperial College London, 5th Floor, Commonwealth Building, Hammersmith Hospital Campus, Du Cane Road, London W12 0NN, United Kingdom; e-mail: j.crawley@imperial.ac.uk.

References

1. Sadler JE. Biochemistry and genetics of von Willebrand factor. Annu Rev Biochem. 1998;67:395-424.
2. Leyte A, Verbeet MP, Brodniewicz-Proba T, Van Mourik JA, Mertens K. The interaction between human blood-coagulation factor VIII and von Willebrand factor: characterization of a high-affinity binding site on factor VIII. Biochem J. 1989;257:679-683.
3. Sadler JE. von Willebrand factor: two sides of a coin. J Thromb Haemost. 2005;3:1702-1709.
4. Haberichter SL, Fahs SA, Montgomery RR. von Willebrand factor storage and multimerization: 2 independent intracellular processes. Blood. 2000;96:1808-1815.
5. Furlan M. Proteolytic cleavage of von Willebrand factor by ADAMTS-13 prevents uninvited clumping of blood platelets. J Thromb Haemost. 2004;2:1505-1509.
6. Zheng X, Chung D, Takayama TK, Majerus EM, Sadler JE, Fujikawa K. Structure of von Willebrand factor-cleaving protease (ADAMTS13), a metalloprotease involved in thrombotic thrombocytopenic purpura. J Biol Chem. 2001;276:41059-41063.
7. Zheng X, Nishio K, Majerus EM, Sadler JE. Cleavage of von Willebrand factor requires the spacer domain of the metalloprotease ADAMTS13. J Biol Chem. 2003;278:30136-30141.
8. Dong JF, Moake JL, Nolasco L, et al. ADAMTS-13 rapidly cleaves newly secreted ultralarge von Willebrand factor multimers on the endothelial surface under flowing conditions. Blood. 2002;100:4033-4039.
9. Dong JF, Moake JL, Bernardo A, et al. ADAMTS-13 metalloprotease interacts with the endothelial cell-derived ultra-large von Willebrand factor. J Biol Chem. 2003;278:29633-29639.
10. Levy GG, Nichols WC, Lian EC, et al. Mutations in a member of the ADAMTS gene family cause thrombotic thrombocytopenic purpura. Nature. 2001;413:488-494.
11. Fujikawa K, Suzuki H, McMullen B, Chung D. Purification of human von Willebrand factor-cleaving protease and its identification as a new member of the metalloproteinase family. Blood. 2001;98:1662-1666.
12. Zhou W, Inada M, Lee TP, et al. ADAMTS13 is expressed in hepatic stellate cells. Lab Invest. 2005;85:780-788.
13. Suzuki M, Murata M, Matsubara Y, et al. Detection of von Willebrand factor-cleaving protease (ADAMTS-13) in human platelets. Biochem Biophys Res Commun. 2004;313:212-216.
14. Shang D, Zheng XW, Niiya M, Zheng XL. Apical sorting of ADAMTS13 in vascular endothelial cells and Madin-Darby canine kidney cells depends on the CUB domains and their association with lipid rafts. Blood. 2006;108:2207-2215.
15. Turner N, Nolasco L, Tao Z, Dong JF, Moake J. Human endothelial cells synthesize and release ADAMTS-13. J Thromb Haemost. 2006;4:1396-1404.
16. Manea M, Kristoffersson A, Schneppenheim R, et al. Podocytes express ADAMTS13 in normal renal cortex and in patients with thrombotic thrombocytopenic purpura. Br J Haematol. 2007;138:651-662.
17. Chion CK, Doggen CJ, Crawley JT, Lane DA, Rosendaal FR. ADAMTS13 and von Willebrand factor and the risk of myocardial infarction in men. Blood. 2007;109:1998-2000.
18. Crawley JT, Lane DA, Woodward M, Rumley A, Lowe GD. Evidence that high von Willebrand factor and low ADAMTS13 levels independently increase the risk of a non-fatal heart attack. J Thromb Haemost. 2008;6:583-588.
19. Dent JA, Berkowitz SD, Ware J, Kasper CK, Ruggeri ZM. Identification of a cleavage site directing the immunochemical detection of molecular abnormalities in type IIA von Willebrand factor. Proc Natl Acad Sci U S A. 1990;87:6306-6310.
20. Tsai HM. Physiologic cleavage of von Willebrand factor by a plasma protease is dependent on its conformation and requires calcium ion. Blood. 1996;87:4235-4244.
21. Furlan M, Robles R, Lamie B. Partial purification and characterization of a protease from human plasma cleaving von Willebrand factor to fragments produced by in vivo proteolysis. Blood. 1996;87:4223-4234.
22. Plaimauer B, Zimmermann K, Volkel D, et al. Cloning, expression, and functional characterization of the von Willebrand factor-cleaving protease (ADAMTS13). Blood. 2002;100:3626-3632.
23. Andreini C, Banci L, Bertini I, Elmi S, Rosato A. Comparative analysis of the ADAM and ADAMTS families. J Proteome Res. 2005;4:881-888.
24. Bode W, Kress LF, Meyer EF, Gomis-Ruth FX. The crystal structure of adamalysin II, a zinc-endopeptidase from the snake venom of the eastern diamondback rattlesnake Crotalus adamanteus. Braz J Med Biol Res. 1994;27:2049-2068.
25. Perutelli P, Amato S, Molinari AC. Cleavage of von Willebrand factor by ADAMTS-13 in vitro: effect of temperature and barium ions on the proteolysis kinetics. Blood Coagul Fibrinolysis. 2005;16:607-611.
26. Anderson PJ, Kokame K, Sadler JE. Zinc and calcium ions cooperatively modulate ADAMTS13 activity. J Biol Chem. 2006;281:850-857.
27. Kokame K, Nobe Y, Kokubo Y, Okayama A, Miyata T. FRETS-VWF73, a first fluorogenic substrate for ADAMTS13 assay. Br J Haematol. 2005;129:93-100.
28. Crawley JT, Lam JK, Rance JB, Mollica LR, O'Donnell JS, Lane DA. Proteolytic inactivation of ADAMTS13 by thrombin and plasmin. Blood. 2005;105:1085-1093.
29. Zanardelli S, Crawley JT, Chion CK, Lam JK, Preston RJ, Lane DA. ADAMTS13 substrate recognition of von Willebrand factor A2 domain. J Biol Chem. 2006;281:1555-1563.
30. Lam JK, Chion CK, Zanardelli S, Lane DA, Crawley JT. Further characterization of ADAMTS-13 inactivation by thrombin. J Thromb Haemost. 2007;5:1010-1018.
31. McKinnon TA, Chion AC, Millington AJ, Lane DA, Laffan MA. N-linked glycosylation of VWF modulates its interaction with ADAMTS13. Blood. 2008;111:3042-3049.
32. Favaloro EJ. Collagen binding assay for von Willebrand factor (VWF:CBA): detection of von Willebrands Disease (VWD), and discrimination of VWD subtypes, depends on collagen source. Thromb Haemost. 2000;83:127-135.
33. Baillod P, Affolter B, Kurt GH, Pflugshaupt R. Multimeric analysis of von Willebrand factor by vertical sodium dodecyl sulphate agarose gel electrophoresis, vacuum blotting technology and sensitive visualization by alkaline phosphatase anti-alkaline phosphatase complex. Thromb Res. 1992;66:745-755.
34. Arnold K, Bordoli L, Kopp J, Schwede T. The SWISS-MODEL workspace: a web-based environment for protein structure homology modelling. Bioinformatics. 2006;22:195-201.
35. Gerhardt S, Hassall G, Hawtin P, et al. Crystal structures of human ADAMTS-1 reveal a conserved catalytic domain and a disintegrin-like domain with a fold homologous to cysteine-rich domains. J Mol Biol. 2007;373:891-902.
36. Mosyak L, Georgiadis K, Shane T, et al. Crystal structures of the two major aggrecan degrading enzymes, ADAMTS4 and ADAMTS5. Protein Sci. 2008;17:16-21.
37. Bode W, Reinemer P, Huber R, Kleine T, Schnierer S, Tschesche H. The X-ray crystal structure of the catalytic domain of human neutrophil collagenase inhibited by a substrate analogue reveals the essentials for catalysis and specificity. EMBO J. 1994;13:1263-1269.
38. Shieh HS, Mathis KJ, Williams JM, et al. High resolution crystal structure of the catalytic domain of ADAMTS-5 (aggrecanase-2). J Biol Chem. 2008;283:1501-1507.